A NEW APPROACH TO PREDICT FOULING USING A TRANSIENT CFD MODEL AND DYNAMIC MESH

Juan N. FLORES-BALDERAS, Jorge A. ALFARO-AYALA, José J. RAMÍREZ-MINGUELA*, Agustín R. URIBE-RAMÍREZ, Oscar A. LÓPEZ-NÚÑEZ

Department of Chemical Engineering, University of Guanajuato, DCNE, Guanajuato, Gto., Mexico

* Corresponding author; E-mail: jdj.ramirezminguela@ugto.mx

In this work, a novel approach to predict the fouling layer growth on the internal surface of a tube by means of a transient computational fluid dynamics model is presented. The transient computational fluid dynamics model takes into account the complexity of the chemical and physical phenomena coupled with dynamic mesh. The dynamic mesh method is programmed by the User Defined Functions for allowing to grow the fouling on the internal surface of the tube. The study is carried out through the computational fluid dynamics in a two dimensions computational domain which contemplates: the radial effects of the profiles of temperature and velocity, and the consumption and productions of species due to chemical reactions. This approach is applied for the fouling deposits on the internal surface of a tube of a petrochemical fired heater, due to the thermal cracking process of oil. Results of the temperature, the oil velocity, the concentration of the distillate and the coke distribution fields are obtained. Moreover, the fouling layer growth, due to the deposit and accumulation along the time, is predicted, and also, the tube metal temperature is computed to identify the "hot spots". According to the results, the fouling layer reduces the diameter of the tube until 24% at the exit in comparison with the clean tube, which leads to the apparition of the "hot spots" due to a high increment of the tube metal temperature at the exit.

Key words: *Fouling, Transient, Computational fluid dynamics, Dynamic mesh, Coke, Thermal cracking*.

1. Introduction

In the industry of oil refining, it is common to use petrochemical fired heaters to make the thermal cracking process. The main objective of this process is to have the oil under high temperatures to increase the production of the middle distillate and light distillate to make more efficiency the process. This process uses residual oil and high temperature to decrease the oil viscosity. The thermal cracking process is carried out to delayed coking or visbreaker, and it depends on the application and the requirements of the process. During the thermal cracking of the oil under high temperatures, a common problem of fouling due to the formation of the coke is encountered. The coke is produced by the reactions like bulk solid coke, and then, the solid coke is added on the internal surface of the tubes of the fired heaters. The accumulation of the fouling layer on the surface of the tube inhibits the

transfer of heat, taking the process to have a state of overheating and to reach the metallurgical temperature limit [1,2].

Nowadays, the power of the hardware and the software of CPUs makes it possible to perform detailed investigations of the combustion of the fired heaters using computational fluid dynamics (CFD). In this sense, just few works consider the thermal cracking studies inside the tubes of the fired heaters, such as: Takatsuka et al. [3] proposed a tubular fouling model for residue cracking furnaces by modeling coke precursor sedimentation. The results were validated with an experimental pilot plant and a commercial unit. Martin and Barletta [1,2] presented two cases of study for thermal cracking of oil of fired heater. They conclude that a fast coking due to operational conditions makes unscheduled stops of the process. Souza et al. [4] developed a CFD numerical model for a single-phase flow inside tubes of fired heaters for the oil refining. The governing equations were solved by the finite volume method. The objective of the work was to obtain the operational conditions to reduce the formation of coke due to the thermal cracking. However, a refinement of the mesh on the internal surface of the tube was not considered, it means that the effects of the boundary layer are missing. Schepper et al. [5] carried out a CFD numerical simulation with Ansys-Fluent®. This work considers a coupled simulation between the gas combustion of the furnace and the thermal cracking with vapor inside the tubes. The model included the transfer of heat by radiation using the Discrete Ordinate Model (DOM). The study was focused mainly to find the flow of species, the temperature and the velocity fields, however, the phenomena of coking inside the tubes is not described. Bayat et al. [6] developed a 2D CFD numerical model to study the behavior of fouling inside the crude oil preheaters. The oil considered is composed by asphaltenes and salt and the chemical reactions were defined by the species transport in the commercial software Ansys-Fluent®. The formation of fouling layer on the internal surface of the tube is missing. Li et al. [7] simulated the thermal cracking of dichloride of ethylene by mean of Matlab. They predicted the coke layer on the internal surface of a coil-reactor along the time. However, the study was carried out in 1D and does not contemplate the radial effects, such as radial profiles of the temperature, the velocity and the species. Fontoura et al. [8] modeled the thermal cracking and phase change on the internal surface of the tube of a fired heater by CFD. The results showed the temperature field and the stream velocities, however, the formation of the fouling layer was not discussed. The previous study was extended by Li et al. [9], they developed a model with three phases gas-liquid-solid in 3D by means of CFD. It was predicted the phase change, the species due to the reactions inside the tube for different types of oil, the temperature fields, the fluid flow, the separation of liquid-gas and the formation of coke, however, the dynamic grow up of the fouling layer on the surface of the tube is not considered. Moreover, Vandewalle et al. [10] developed a dynamic simulation of fouling in steam cracking reactor using CFD for three-dimensional coil geometries, their 3D dynamic mesh proposal is based on the calculation of the extrusion distance using a specific extrusion model, and it is worth to mentioning that the governing equations for a compressible, reactive, single-phase fluid flow were considered in steady-state conditions.

More recent works [11–14] have concentrated their efforts on improving the prediction models of fouling by various precursors in heat exchange equipment, considering various techniques, however, these are not considering the dynamic formation of the fouling layer as a solid domain, therefore, for high temperature processes, it is not possible to evaluate the real effect of the temperature on the surface of the tubes and, consequently, it is not possible to compute the operating time in which the metallurgical temperature limit is reached. Therefore, in this work, a study of the

deposition of a fouling layer on the internal surface of a tube of a petrochemical fired heater due to the thermal cracking process of oil is presented. The study is carried out through a transient computational fluid dynamics model (CFD) in a 2D computational domain. The accumulation of coke and the fouling layer that is growing up on the internal surface of a tube of a fired heater are obtained. The fouling layer on the internal surface of the tube is predicted by the complexity of the chemical and physical phenomena coupled by the dynamic mesh technique. The dynamic mesh method is programmed by the User Defined Functions (UDFs) for allowing the growing up of the fouling layer on the internal surface of the tube. The modeling of the fouling layer on the internal surface of the tube allows predicting the temperature on the surface of the tube, known as the tube metal temperature (TMT), in consequence, it is possible to identify the "hot spots" and the temperatures that are close to the metallurgical temperature limit. Furthermore, the model used in this work predicts the maximum operational time (run-length), according to the international standards for the design of the thermal cracking process of the oil in the fired heaters for the refining industry. Finally, a detailed prediction of the fouling layer is achieved with this new approach, and it considers: the dynamic mesh through computational fluid dynamics, the thickness of the fouling layer with the effects of the tube metal temperature, the hydrodynamics of the flow, chemical reactions and mass transfer.

2. CFD model

The developed model to predict the formation of the coke and the accumulation of the fouling layer on the internal surface of the tube of a fired heater considers the oil represented by saturated, aromatic, resins, asphaltenes (S.A.R.A.) and the products of the chemical reaction as the distillate, asphaltenes in mesophase and coke. The asphaltenes in mesophase and coke are considered as microscopic particles that are in the fluid flow, and they do not affect the chemical kinetics used, the deposition of the fouling layer and the progressive growing up depend of the concentration of the coke that is located on the viscous sublayer in the hydrodynamic boundary layer.

2.1. Governing equations

The thermal cracking of the oil considers a group of seven pseudo-components according to the chemical kinetics by Köseoglu and Phillips [8,15-18].

$$S_{Distillate} = k_1 Y_{sat} \rho \quad (1)$$

$$S_{Saturates} = k_2 Y_{arom} \rho - k_1 Y_{sat} \rho \quad (2)$$

$$S_{Aromatics} = k_3 Y_{res} \rho - k_2 Y_{arom} \rho \quad (3)$$

$$S_{Resins} = k_5 \left(Y_{asphsol} + Y_{asphmeso}\right) \rho - (k_3 + 2k_4) Y_{res} \rho \quad (4)$$

$$S_{Soluble\ Asphaltenes} = k_4 Y_{res} \rho - k_5 Y_{asphsol} \rho \quad (5)$$

$$S_{Asphaltenes\ in\ Mesophase} = k_4 Y_{res} \rho - (k_5 + k_6) Y_{asphmeso} \rho \quad (6)$$

$$S_{Coke} = k_6 Y_{asphmeso} \rho \quad (7)$$

The reaction rate constants, k_i, are obtained by Arrhenius [8]:

$$k_i = A\ exp(-E/RT) \quad (8)$$

Table 1. Chemical reaction constants.

Reaction	A (s^{-1})	E (J/mol)
1	2.686×10^9	175,000
2	4.161×10^6	136,000
3	217.3	85,000

4	7,196	96,000
5	69,655	103,000
6	2.536×10^8	168,000

The constants of frequency factor *A* and energy activation *E* are given in the la Tab. 1.

The mass conservation equation, or continuity equation, is expressed as follows:

$$\partial\rho/\partial t + \nabla \cdot \rho\vec{v} = 0 \tag{9}$$

The conservation of the species, pseudo-components, Y_i, are solved by the species transport model.

$$\partial(\rho Y_i)/\partial t + \nabla \cdot (\rho\vec{v}Y_i) = \nabla \cdot [(\mu + \mu_t)\nabla Y_i] + S_i \tag{10}$$

The rates of creation and consumption of the species or pseudo-components are introduced in the model as source terms, S_i. The conservation of momentum in an inertial reference frame is described by [6]:

$$\frac{\partial}{\partial t}(\rho\vec{v}) + \nabla \cdot (\rho\vec{v}\vec{v}) = -\nabla p + \nabla \cdot [(\mu + \mu_t)\nabla \cdot \vec{v}] \tag{11}$$

To compute the turbulence viscosity, μ_t, it was used the shear-stress transport (SST) *k*-*ω* model due to the accuracy and numerical stability [19]. The turbulent kinetic energy *k* and turbulent frequency *ω* are computed by the following relations:

$$\frac{\partial}{\partial t}(\rho k) + \nabla \cdot (\rho\vec{v}k) = \nabla \cdot \left[\left(\mu + \frac{\mu_t}{\sigma_k}\right)\nabla k\right] + G_k - Y_k \tag{12}$$

$$\frac{\partial}{\partial t}(\rho\omega) + \nabla \cdot (\rho\vec{v}\omega) = \nabla \cdot \left[\left(\mu + \frac{\mu_t}{\sigma_\omega}\right)\nabla\omega\right] + G_\omega - Y_\omega \tag{13}$$

where G_k and G_ω are production terms of k and ω, and Y_k and Y_ω represent the destruction rates. σ_k and σ_ω are also the turbulent Prandtl numbers for k and ω, respectively. The μ_t is computed as:

$$\mu_t = \alpha^* \rho \frac{k}{\omega} \tag{14}$$

The coefficient α^* damps the turbulent viscosity causing a low-Reynolds-number correction. The phenomena that are governed by the transfer of heat in the tube is calculated by:

$$\frac{\partial}{\partial t}(\rho E) + \nabla \cdot (\rho\vec{v}E) = -\nabla p + \nabla \cdot \left(k_{eff}\nabla T\right) \tag{15}$$

where k_{eff} is the effective thermal conductivity $(k + k_t)$, and k_t is the turbulent thermal conductivity.

2.2. Fouling of coke model

The model is base under the approach of Kern and Seaton [20-22], where the net fouling rate is the difference between the rate of deposition and the rate of removal and it is the result of the equilibrium between the forces developed in the flow. Under this method, it is possible to establish a reaction-transport model and a fouling rate, also known as coking rate, X_{cr}, calculated as:

$$X_{cr} = \rho K_c Y_{coke} \tag{17}$$

where K_c is the global mass transfer coefficient.

The coke is deposited and accumulated on the internal surface of tube to develop a fouling layer and it is assumed that it adheres strongly in such a way that the amount of fouling can not be removed by diffusion or shear stresses due to the lower velocities. The global mass transfer coefficient can be obtained by the analogy of convection heat-mass and then the use of the Sherwood number relationships for fully developed flow in smooth circular tubes and turbulent flow [24] is defined as following:

$$Sh = 0.023 Re^{0.8} Sc^{0.4} \quad Re > 10{,}000 \quad 0.7 < Sc < 160 \tag{18}$$

Then, the global mass transfer coefficient is obtained from the Sherwood number definition, K_c:

$$K_c = \frac{ShD_i}{D} \tag{19}$$

where D is the diameter of the tube and D_i is the coefficient of the mass diffusivity for turbulent flow, it is related to the effective viscosity, μ_{ef}, and the density of the oil, ρ:

$$D_i = \frac{\mu_{ef}}{\rho} \tag{20}$$

$$\mu_{ef} = \mu + \mu_t \tag{21}$$

The fouling layer is defined as:

$$\Delta\varepsilon_{fl}(x) = \frac{X_{cr}(x)}{\rho_{fl}}\Delta t \tag{22}$$

where ρ_{fl} is the density of the fouling layer.

2.3. Numerical simulations

The delayed coking process included the phenomenon of fouling of solid coke that is formed on the internal surface of the tube of a fired heater. According to Martin and Barletta [1,2], the fired heater should be turn off to clean the tubes by removing the coke that is added on the internal surface of the tube, when the temperature of the metal tube (TMT) reaches 950 K. This temperature corresponds to the metallurgical limit supported by stainless steel TP304L SS (18Cr-8Ni), and it is used in this work. The numerical simulations were carried out in an unsteady state, it is used due to the coking rate is slow in comparison to the coke that is obtained from the rate of the chemical reactions. A time step analysis based on the total mass of fouling deposited on the tube wall was performed considering different time steps, and it was found that 6 hours had a good result. A 2D computational domain and dimensions of 25 m of length and 0.1524 m of diameter were considered. A mesh sensitivity analysis with structured meshes of 210,000, 261,000, 384,000, 420,000 and 480,000 quadrilateral elements were tested. It was observed that the results no longer varied for the 420,000 elements mesh. The mesh was refined near the tube wall in order to consolidate the calculation in the viscous sublayer of the boundary layer region, since it is assumed that the formation of the fouling layer is develop near the wall. The meshing is done by Ansys-Meshing®. It was stablished a boundary condition of "velocity inlet" at the entrance of the tube with a fully developed velocity profile, it was defined by a User Defined Function (UDF) and its average velocity value is 2 m/s. Also, the oil temperature is 673 K (400 ºC) at the inlet and the mass fraction of the pseudo-components of the vacuum residuum (VR) of Arabian light crude oil is shown in the Tab. 2.

Table 2. Chemical reaction constants.

Pseudo-components	Y_i
Distillate	0.00
Resins	0.32
Saturates	0.18
Aromatics	0.34
Asphaltenes	0.16
Mesoasphaltenes	0.00
Coke	0.00

A boundary condition of pressure outlet was used considering the atmospheric pressure at the outlet of the tube. A constant value of 88,329 W/m^2 of a maximum heat flux at the walls of the tube was considered. This value is recommended to evaluate the coking potential according to Martin and

Barletta [1,2]. The properties of the fluid such as density, viscosity, specific heat and thermal conductivity, are shown in Eq. (23-26), respectively.

$$\rho = 1.7768 \cdot 10^{-6} \cdot T^2 - 5.3905 \cdot 10^{-1} \cdot T + 1173.7 \quad (23)$$

$$\mu = \left[10^{10^{(A-B \cdot log(T))}} - 0.7\right] \cdot 10^{-6} \cdot \rho \quad (24)$$

$$c_p = 1.4191 \cdot 10^{-5} \cdot T^2 + 3.0126 \cdot T + 785.8 \quad (25)$$

$$k = -1.9482 \cdot 10^{-9} \cdot T^2 - 5.6777 \cdot 10^{-5} \cdot T + 0.1298 \quad (26)$$

In Eq. (24) A and B are constants of the fluid, which in this case for the vacuum residuum (VR) of Arabian light crude oil are 37.2564 and 14.2007, respectively. The fouling layer formed on the internal surface of the tube has its own properties as solid material, these are considered as constants as following: the density ρ_{fl} is 1,600 kg/m^3 [25], the specific heat $c_{p,fl}$ is 1,500 J/kgK [6] and the thermal conductivity k_{fl} is 6.46 W/mK [25].

The Dynamics Mesh Method of the Ansys-Fluent® allows the growing up of the mesh and it is controlled with User Define Functions (UDFs), the growing up of the mesh is according the growing up of the fouling layer (fouling) developed on the internal surface of the tube. The mesh grows up on the internal surface of the tube as a solid domain while the fluid domain decreases, the mesh of the fluid domain absorbs this movement of the solid domain distributing the cells of the fluid domain, so that the solution and the convergence is achieved with the dynamics mesh. Under the *k-ω* model (SST) approach, 10 structured cells within the boundary layer are needed. For this reason and taking into account that the dynamic mesh of the fluid domain is refined as the simulation runs. The y^+ is around 0.2, ensuring that the first cell lies within the viscous sublayer (y^+<1).

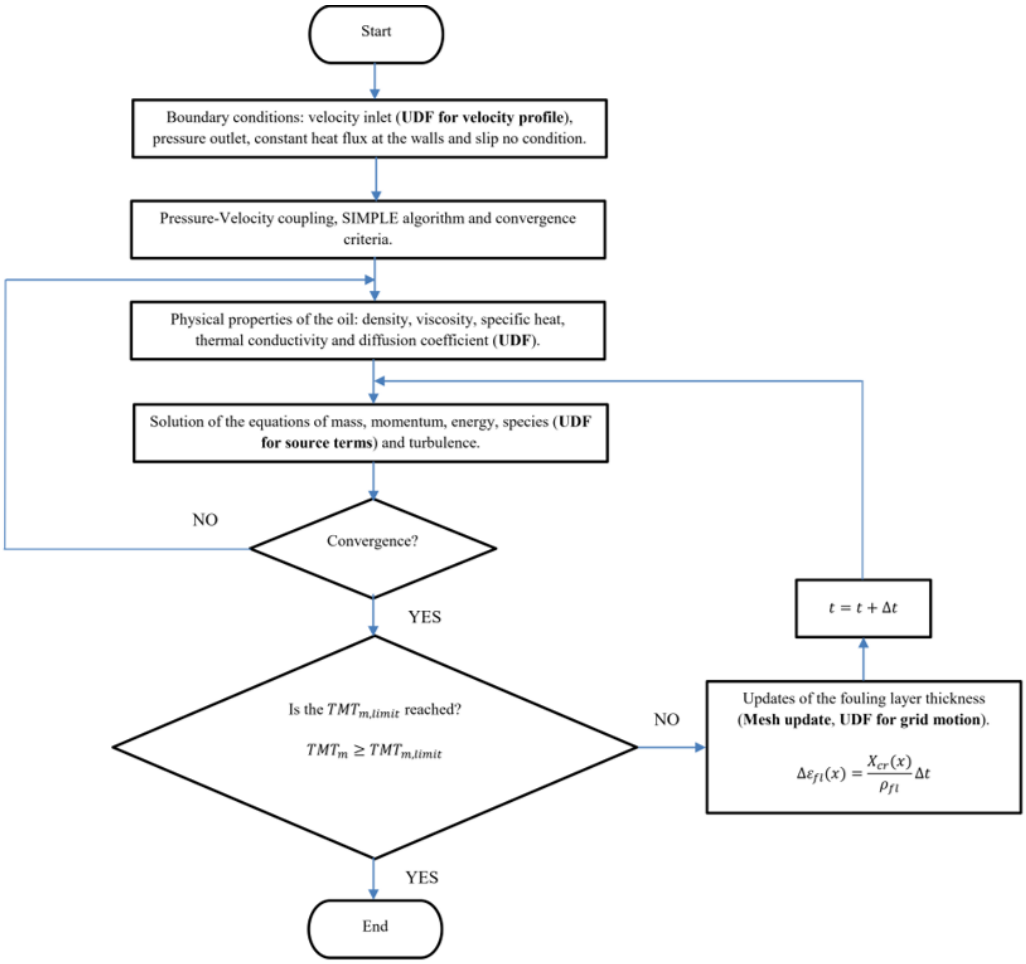

Figure 1. Algorithm of the thermal cracking process

The continuity equation, the momentum equation, the turbulence model, the species transport model, the energy equation, and the chemical kinetic model are used to obtain the solution of the thermal cracking of oil. The SIMPLE algorithm is considered for the pressure-velocity coupling. The discretization schemes of second order are used. A relaxation factor of 0.3 is used for most of the variables to achieve the solution convergence. Scaled residuals are monitored for all the variables and the solution is converged when the residuals are lower than 10^{-6}. Once the solution converges, the coke fouling model is coupled with the dynamic mesh, programmed by a UDF to control the increase and decrease of the solid and fluid domain mesh cells, respectively. The algorithm of the thermal cracking process is shown in Fig. 1.

3. Results and discussion

The validation of the numerical model was made with the reported experimental data in the literature. The velocity profile was modeled on Ansys-Fluent®, and the estimated dimensionless results were compared by the CFD model with the experimental results [4,8], it was in a good concordance, see Fig. 2, with a maximum percent error of 6.8%.

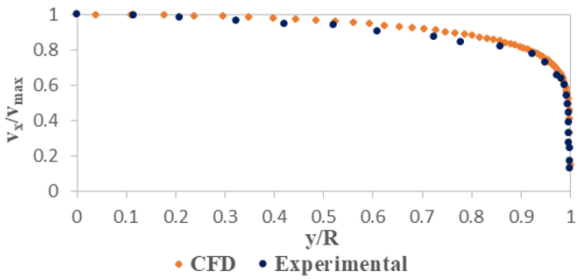

Figure 2. Comparison of the velocity profile estimated by the CFD and experimental data for turbulent fluid flow (Re = 500,000)

Also, the pressure drop obtained by CFD for different Reynolds was compared with the pressure drop obtained by the equation derived from the Moody friction factor [4]. The CFD numerical results shows a maximum percent error of 1.2%, see Fig. 3.

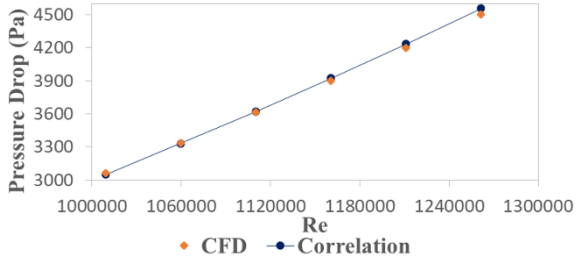

Figure 3. Comparison of the pressure drop by CFD and the correlation for the turbulent flow

The contours of the oil temperature along the tube are illustrated in Fig. 4. It shows that the heat transfer to the center of the tube occurs such that the thermal entry zone is achieved at a length of 2 m. Since the heat transfer takes place from the tube wall to the fluid, a maximum temperature of 689.5 K at the exit of the tube is reached near the wall. The average temperature of the oil increases from the entrance of 673 K to the exit of the tube at 679.3 K, this is due to the heat transfer rate to the center of the tube, where the effect of the thermal boundary layer is important, since the heat transfer occurs from the tube wall to the flowing oil.

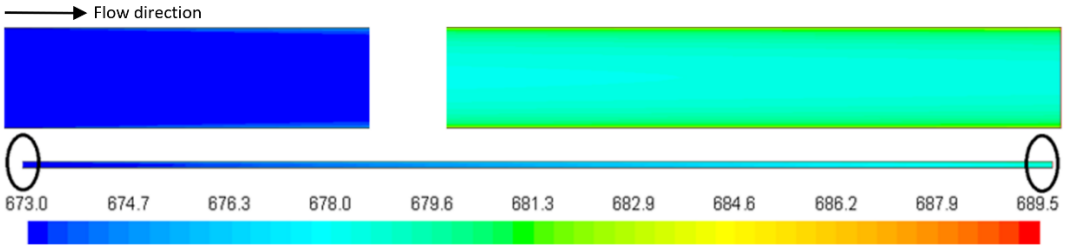

Figure 4. Profile and contours of the oil temperature

Figure 5 shows the profile and contours of the mass fraction of the coke, it can be observed that a high dependence of the formation of coke and the temperature of the oil. The increase of the coke is obtained by the chemical kinetic. The mass fraction of the coke is higher near the internal surface throughout the tube in comparison with the central zone of the tube, this is due to the exponentially increasing reaction rate constants, and these constants depend on temperature, Fig. 4.

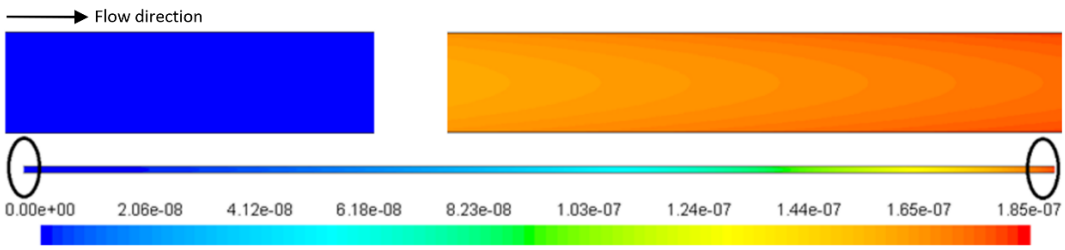

Figure 5. Profile and contours of the mass fraction of the coke

Figure 6 shows the profile and the contours of the distillate. It is observed that the mass fraction of the distillate is increasing from the entrance to the exit of the tube due to the increment of the temperature along the tube, see Fig. 4.

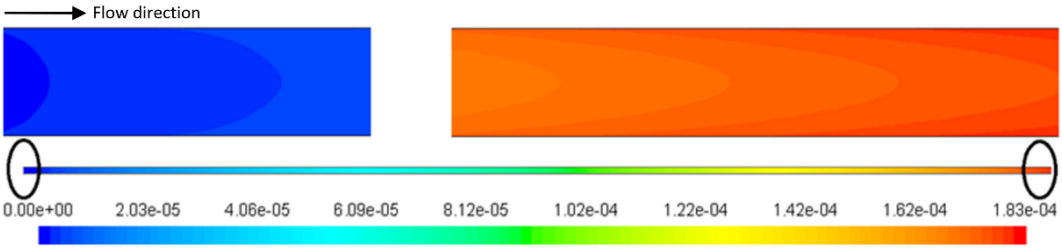

Figure 6. Profile and contours of the mass fraction of the distillate

Approximately 990 times more distillate than coke is produced, see Fig. 5 and Fig. 6. This properly demonstrates the viability of the processes, therefore, the distillate formation is faster compared to coke formation, this is due to the distillate depends directly of the amount of the aromatics and saturates. This phenomenon was expected, and it is due to the mass fraction of the pseudo-components that was introduced at the entrance of the tube to characterize the vacuum residuum (VR) of Arabian light crude oil and the kinetic of thermal cracking.

The growing up of the fouling layer on the internal surface of the tube is shown in the Fig. 7, it can be observed for the time of 8 and 16.8 months.

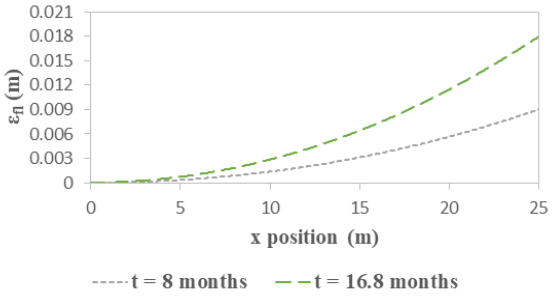

Figure 7. Fouling layer growing up

The behaviour of the increment of the fouling layer is exponential due to it depends of the concentration of the coke inside the viscous sublayer. A maximum thickness of fouling layer of 0.018 m at the time of 16.8 months when the limit maximum tube metal temperature is obtained, at the exit of the tube. The diameter of the tube is reduced from 0.1524 m at the entrance of the tube to 0.1164 m at the exit of the tube, approximately a reduction of 24%. This behaviour makes the fluid flow of the oil to increase its velocity due to the reduction of the cross-sectional section. The oil mass flux rate remains constant for the beginning of the process because there is no fouling layer, and the cross-sectional section is constant in the tube. For the following operational times, the oil mass flux rate remains constant form the entrance of the tube to around a length of 5 m due to the thickness of fouling layer has reached a maximum value of 0.001 m, this has an insignificant impact on the increase in oil velocity and therefore in the oil mass flux rate. Above a length of 5 m of the tube, the oil mass flux rate increases exponentially due to the increase of the thickness of fouling layer (reduction of the cross-sectional section). At the time of 16.8 months, the maximum value of 2,190 $kg/m^2 \cdot s$ of oil mass flux rate was reached at the exit of the tube, see Fig. 8.

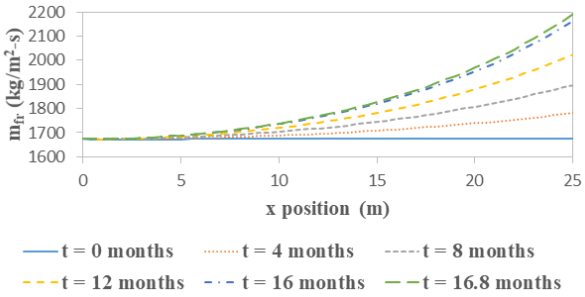

Figure 8. Oil mass flux rate profiles

The oil film temperature (oil-fouling layer interface temperature) along the tube for different operational time is shown in Fig. 9. It can be observed that from 0 m to 5 m of the length of the tube, the film temperature increases similarly for all the operational time. Also, it is observed that fluctuations appear throughout the operational time, these fluctuations of the film temperature depend of the interaction between the thermal resistance for convection and the thermal resistance for conduction due to the reduction of the cross-sectional section and the increment of the fouling layer, respectively. For a higher operational time than 12 moths, the film temperature decreases near to the exit of the tube due to the oil mass flux rate reaches a value of approximately 2,000 kg/m^2·s. The oil film temperature decreases until the thermal resistance for convection and conduction are equal, this behaviour allows increasing the run-length. It is due to the velocity of the oil increasing (decreasing the residence time) and the convective heat transfer coefficient is improved, consequently the film temperature decreases.

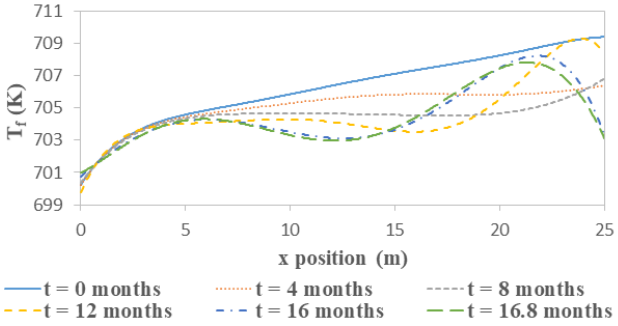

Figure 9. Oil-fouling layer interface temperature profiles (oil film temperature)

Coking rate profiles are shown in the Fig. 10. It is shown that the coking rate is an exponential function of the oil film temperature and the reaction rate as it was expected. Also, the coking rate increases along the tube due to the mass fraction of the coke increases, see Fig. 5, and it decreases along the operational time due to the coke decreases due to the average oil film temperature decreases (706.3 K, 704.5 K and 703.5 K, for 0, 8 and 16.8 months respectively).

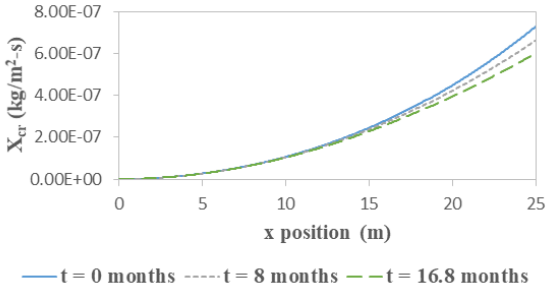

Figure 10. Coking rate profiles

The tube metal temperature (TMT) along the x-direction of the tube and the operational time is shown in Fig. 11. The TMT increases due to the fouling layer is growing up on surface of the tube (see Fig. 7), it has a behavior like an insulator material. The TMT increases along the tube and the operational time. The increment of the TMT is due to the mass fraction of the coke in the viscous sublayer increases, the coking rate increases and the fouling layer grows up. The maximum tube metal temperatures are 709.7 K, 770.2 K, 829.5 K, 886.3 K, 939.8 K and 949.7 K for 0, 4, 8, 12, 16, and 16.8 months, respectively, at the exit of the tube.

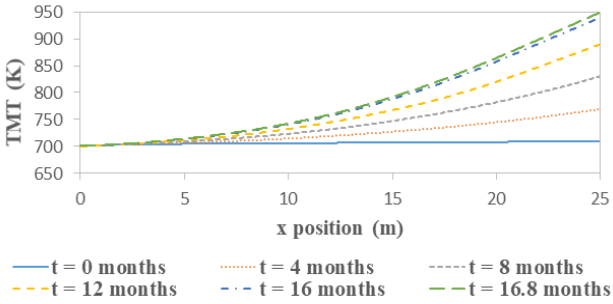

Figure 11. Tube metal temperature profiles (TMT)

The maximum tube metal temperature, TMT_m, represents a "hot spot" that is reached at the exit of the tube, see Fig. 12. A operational time of 16.8 months is enough to reach the $TMT_{m,limit}$ of 950 K. This time is inside the interval operation of a typical fired heater for the delayed coking [1].

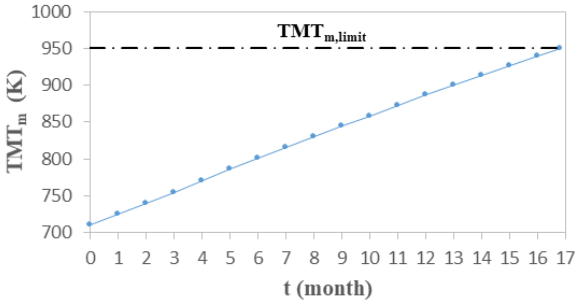

Figure 12. Maximum tube metal temperature vs the time at the exit of the tube

Contours of the velocity and temperature are shown in the Fig. 13 and Fig. 14, respectively, these are for 0, 8 and 16.8 months. The deposition and accumulation of the fouling layer on the internal surface of the tube is achieved with the dynamics mesh that represents the growing up of the solid domain. This growing up of the fouling layer decreases the cross-sectional section along the tube

and this provokes an increment of the average velocity, due to the conservation of mass. At the exit of the tube, the average velocity is 2.05 m/s at the starting of the operation and then the velocity is 2.69 m/s at the operational time of 16.8 months. Similarly, the maximum velocity, is 2.2 m/s in the central zone of the fluid flow at the starting of the operation of the tube of the fired heater and then the maximum velocity is 2.86 m/s at the operational time of 16.8 months.

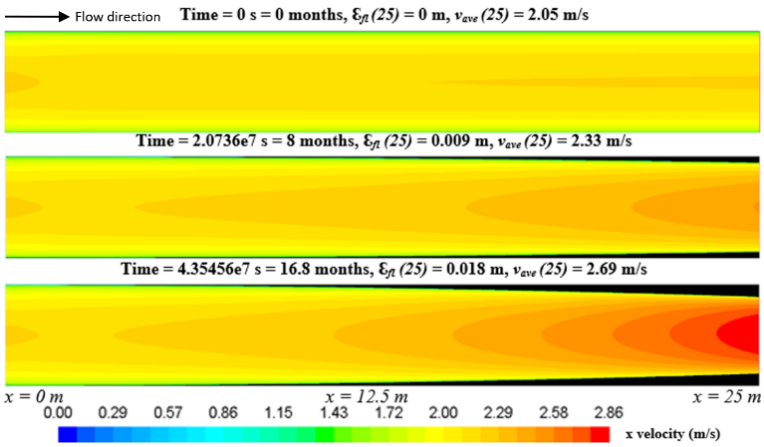

Figure 13. Velocity contours at the tube along the operational time

The average temperature of the oil increases from the entrance of 673 K to the exit of the tube of 679.3 K, it is an increment of 6.3 K, this value keeps constant along the operational time due to the conservation of energy, see Fig. 14. The temperature contours show the increment of the temperature gradient inside the fouling layer along the operational time of the fired heater. The gradient profile presents a linear behavior due the tube is studied as a two-dimensional 2D model and that the properties for the fouling layer are considered constant.

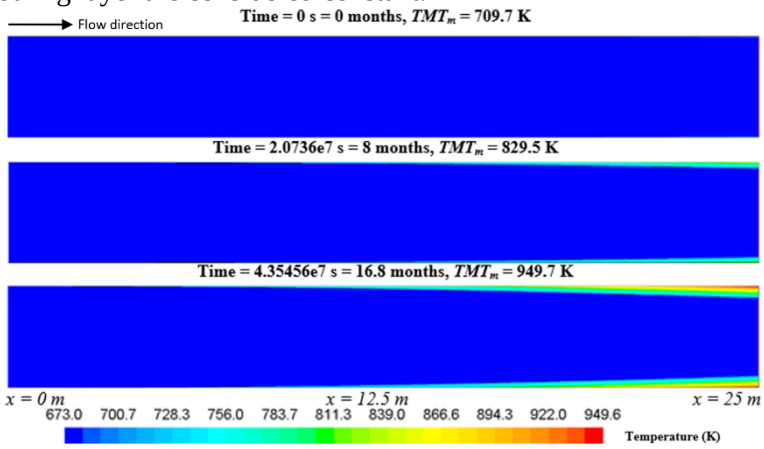

Figure 14. Temperature contours at the tube along the operational time

4. Conclusions

The formation of coke, the deposition of solid coke and the progressive growing up of the fouling layer was studied in this work. The main conclusions are:

- The dynamics meshes make that the solid domain grows up according to the chemical reactions, the chemical kinetics, the heat and mass transfer and the coke located in the viscous sublayer of the boundary layer of the fluid flow.
- The increment o decrement of the fouling rate depends directly on the oil film temperature, the concentration of the foulant (coke) in the boundary layer and the equilibrium between the forces developed in the flow.
- An fouling layer of 0.018 m makes to reach the temperature of the metal tube limit, $TMT_{m,limit}$ ("hot spot"), of 950 K in an operational time of 16.8 months.
- Due to the interaction that occurs between the reduction of the cross-sectional section, the thermal resistances for convection (pseudo-components) and conduction (fouling layer) and the mass flux rate, it is recommended that the fired heaters operate under an oil mass flux rate equal or higher than 2,000 kg/m^2·s, in order to decrease oil film temperature, the formation of coke in the viscous sublayer and the coking rate. These allow increasing the run-length to obtain more valuable products and minimizes the overheating of the metal tube and the risk of failure.

Finally, this work gives a novel approach with the use of the computational fluid dynamics to predict the formation and growing up of the fouling layer on the internal surface of the tube by a detailed description of the phenomenon involved.

Acknowledgements

The authors gratefully acknowledge to the National Council of Science and Technology (CONACYT), Mexico, for financial support of an educational scholarship to J. Nicolás Flores-Balderas, for the SNI program and for the financial support under the *"Proyecto Apoyado por el Fondo Sectorial de Investigación para la Educación", I1200/169/2019 MOD.ORD./38/2019 "FONDO SECTORIAL DE INVESTIGACIÓN PARA LA EDUCACIÓN" CB2017-2018 GENERAL A1-S-9539.*

Nomenclature

A, E	– Characteristic parameters for the reactions
C_{coke}	– Coke concentration [kg m^{-3}]
c_p	– Fluid specific heat [J kg^{-1} K^{-1}]
$c_{p,fl}$	– Fouling layer specific heat [J kg^{-1} K^{-1}]
D	– Tube diameter [m]
D_i	– Mass diffusion coefficient *i* [m^2 s^{-1}]
G_k	– Production rate of *k* [kg m^{-1} s^{-3}]
G_ω	– Production rate of ω [kg m^{-3} s^{-2}]
h	– Heat transfer coefficient [W m^{-2} K^{-1}]
k	– Fluid thermal conductivity [W m^{-1} K^{-1}]
K_c	– Global mass transfer coefficient [m s^{-1}]
k_{fl}	– Fouling layer thermal conductivity [W m^{-1} K^{-1}]
k_{eff}	– Thermal effective conductivity [W m^{-1} K^{-1}]
k_t	– Turbulent thermal conductivity [W m^{-1} K^{-1}]
k_{1-6}	– Reaction rate constants [s^{-1}]
T_f	– Film temperature of fluid [K]
TMT	– Tube metal temperature [K]
TMT_n	– Maximum tube metal temperature [K]
$\vec{v}$	– Velocity [m s^{-1}]
x	– *x* position [m]
X_{cr}	– Coking rate [kg m^{-2} s^{-1}]
y	– *y* position [m]
Y_i	– Mass fraction *i* [–]
Y_k	– Destruction rate of *k* [kg m^{-1} s^{-3}]
Y_ω	– Destruction rate of ω [kg m^{-3} s^{-2}]
y^+	– *y*-plus [–]

Greek symbols

$\Delta\varepsilon_{fl}$	– Fouling layer thickness increment [m]

m_{fr}	– Mass flow rate [kg m^{-2} s^{-1}]	ε_{fl}	– Fouling layer thickness [m]
p	– Pressure [Pa]	μ	– Viscosity [Pa s]
R	– Universal gas constant [J mol^{-1} K^{-1}]	μ_{ef}	– Effective viscosity [Pa s]
Re	– Reynolds number ($= \rho v D/\mu$) [–]	μ_t	– Turbulent viscosity [Pa s]
Sc	– Schmidt number [–]	ρ	– Fluid density [kg m^{-3}]
Sh	– Sherwood number [–]	ρ_{fl}	– Fouling layer density [kg m^{-3}]
S_i	– Species source term [kg m^{-3} s^{-1}]	σ_k	– Turbulent Prandtl number for k [–]
t	– Time [s]	σ_ω	– Turbulent Prandtl number for ω [–]
T	– Temperature [K]	ω	– Specific dissipation rate [s^{-1}]

References

[1] Martin, G. R., Vacuum unit fired heater coking - avoid unscheduled shutdowns, *Proceedings*, Process Consulting Services Inc., Houston, U.S.A., 2001, Vol. 1, pp. 1-6

[2] Barletta, T., Why vacuum unit fired heaters coke, *Proceedings*, Process Consulting Services Inc., Houston, U.S.A., 2002, Vol. 4, pp. 123-127

[3] Takatsuka, T., *et al.*, A tubular fouling model for residue cracking furnaces, *J Chem Eng Japan, 22* (1989), 2, pp. 149-154

[4] Souza, B. A., *et al.*, Predicting coke formation due to thermal cracking inside tubes of petrochemical fired heaters using a fast CFD formulation, *J Pet Sci Eng, 51* (2006), 1, pp. 138-148

[5] Schepper, S. C. K., *et al.*, Coupled simulation of the flue gas and process gas side of a steam cracker convection section, *AIChE J, 55* (2009), 11, pp. 2773-2787

[6] Bayat, M., *et al.*, CFD modeling of fouling in crude oil pre-heaters, *Energy Convers Manag, 64* (2012), 1, pp. 344-350

[7] Li, C., *et al.*, Coke deposition influence based on a run length simulation of a 1,2-dichloroethane cracker, *Ind Eng Chem Res, 52* (2013), 49, pp. 17501-17516

[8] Fontoura, D. V. R., *et al.*, A three-dimensional two-phase flow model with phase change inside a tube of petrochemical pre-heaters, *Fuel, 110* (2013), 1, pp. 196-203

[9] Li, X. G., *et al.*, CFD modeling of phase change and coke formation in petroleum refining heaters, *Fuel Process Technol, 134* (2015), 1, pp. 18-25

[10] Vandewalle, L. A., *et al.*, Dynamic simulation of fouling in steam cracking reactors using CFD, *Chemical Engineering Journal, 329* (2017), 1, pp. 77-87

[11] Valus, M. G., *et al.*, Computational fluid dynamic model for the estimation of coke formation and gas generation inside petrochemical furnace pipes with the use of a kinetic net, *Can J Chem Eng, 95* (2017), 12, pp. 2286-2292

[12] Diaz, E., *et al.*, Modeling and prediction of shell-side fouling in shell-and-tube heat exchangers, *Heat Transf Eng, 40* (2019), 11, pp. 845-861

[13] Borges, C., *et al.*, Dynamic analysis of fouling buildup in heat exchangers designed according to TEMA standards, *Ind Eng Chem Res, 57* (2018), 10, pp. 3753-3764

[14] Geerts, M., *et al.,* Crude to olefins: effect of feedstock composition on coke formation in a bench-scale steam cracking furnace, *Ind Eng Chem Res, 59* (2020), 7, pp. 2849-2859

[15] Köseoğlu R. Ö, Phillips C. R, Effect of reaction variables on the catalytic hydrocracking of Athabasca bitumen. Fuel, *67* (1988), 9, pp. 1201-1204

[16] Köseoğlu R. Ö, Phillips C. R., Hydrocracking of Athabasca bitumen: kinetics of formation of gases, *Fuel, 67* (1988), 4, pp. 552-556

[17] Köseoğlu R. Ö, Phillips C. R., Kinetics and product yield distributions in the $CoOMoO_3Al_2O_3$ catalysed hydrocracking of Athabasca bitumen, *Fuel, 67* (1988), 10, pp. 1411-1416

[18] Köseoğlu, R. Ö., Phillips, C. R., Kinetic models for the non-catalytic hydrocracking of Athabasca bitumen, *Fuel, 67* (1988), 7, pp. 906-915

[19] Menter, F. R., Two-equation eddy-viscosity turbulence models for engineering applications, *AIAA J, 32* (1994), 8, pp. 1598-1605

[20] Kern, D. Q., Seaton, R. E., A theoretical analysis of thermal surface fouling, *Br Chem Eng*, *4* (1959), 5, pp. 258-262

[21] Müller, H., Heat transfer fouling: 50 years after the Kern and Seaton model, *Heat Transf Eng*, *32* (2011), 1, pp. 1-13

[22] Deshannavar, U. B., *et al.*, Crude oil fouling: a review, *J Appl Sci*, *10* (2010), 24, pp. 3167–3174

[23] Bennett, C. A., A theory describing asphaltene adhesion fouling inside heat exchanger tubes, *Heat Transf Eng*, *33* (2012), 15, pp. 1246-1250

[24] Taler, D., Taler, J., Simple heat transfer correlations for turbulent tube flow, *Proceedings*, E3S Web Conf., Cracow, Poland, 2017, Vol. 13, pp. 1-7

[25] Plehiers, P. M., *et al.*, Simulation of the run length of an ethane cracking furnace, *Ind Eng Chem Res, 29* (1990), 4, pp. 636-641

Received: 06.12.2021.
Revised: 04.04.2022.
Accepted: 24.05.2022.